Original Investigation

Outer Retinal Corrugations in Age-Related Macular Degeneration

Sotaro Ooto, MD; Sritatath Vongkulsiri, MD; Taku Sato, MD; Mihoko Suzuki, MD; Christine A. Curcio, PhD; Richard F. Spaide, MD

Supplemental content at jamaophthalmology.com

IMPORTANCE Optical coherence tomography (OCT) abnormalities of age-related macular degeneration (AMD) have not been fully characterized because of the complex morphology and a lack of correlative histologic studies. Expansion of our ability to interpret increasing attributes brings us closer to the goal of in vivo histologic analysis of the eye by OCT.

OBJECTIVE To describe a new outer retinal finding of AMD using spectral-domain (SD) OCT and suggest histopathologic correlates.

DESIGN, SETTING, AND PARTICIPANTS Twenty-five eyes of 16 patients with AMD with severe atrophy due to either choroidal neovascularization (CNV) or geographic atrophy (GA) and 53 donor eyes of 53 patients with late AMD were included. Imaging studies were conducted at a referral retinal practice and histopathology was done at a university research laboratory.

EXPOSURES Findings in the outer retina were evaluated in SD-OCT images in eyes with atrophy of the retinal pigment epithelium (RPE) and compared with histopathologic findings in eyes with GA or CNV that also showed loss of the RPE.

MAIN OUTCOMES AND MEASURES Spectral-domain OCT and histologic characteristics of the outer retina.

RESULTS The mean (SD) age of the 16 patients was 82.7 (7.9) years. Twenty eyes had CNV and 5 eyes had GA. The mean best-corrected visual acuity was 0.800 logMAR (interquartile range, 0.350-1.000 logMAR), a Snellen equivalent of 20/126. A curvilinear hyperreflective density was identified above the Bruch membrane line within the atrophic area in the SD-OCT images. At the internal border, the material was contiguous with the outer portion of the RPE band. Below the material was a relatively hyporeflective space. The material was thrown into folds in cases with atrophy following CNV or was seen as a sheet with numerous bumps in eyes with GA. Review of histopathologic findings of eyes with advanced GA and CNV revealed a rippled layer of basal laminar deposits in an area of RPE atrophy that was located in the same level as the curvilinear line seen in the OCT images.

CONCLUSIONS AND RELEVANCE We have described a new entity, termed *outer retinal corrugations*, which may correspond to histological findings of basal laminar deposits, extracellular deposits that persist in eyes with late AMD. Observation of this undulating band does not necessarily mean there is exudation or leakage; as a consequence, these patients do not need treatment based on this solitary finding.

Author Affiliations: LuEsther T. Mertz Retinal Research Center, New York, New York (Ooto, Vongkulsiri, Sato, Suzuki, Spaide); Vitreous Retina Macula Consultants of New York, New York (Ooto, Vongkulsiri, Sato, Suzuki, Spaide); EyeSight Foundation of Alabama Vision Research Laboratories, Department of Ophthalmology, University of Alabama School of Medicine, Birmingham (Curcio).

Corresponding Author: Richard F. Spaide, MD, Vitreous Retina Macula Consultants of New York, 460 Park Ave, 5th Flr, New York, NY 10022 (rick.spaide@gmail.com).

Age-related macular degeneration (AMD) has been the leading cause of severe impairment of visual function in aging people in industrialized countries. One manifestation of late AMD is geographic atrophy (GA), an area of focal loss of the retinal pigment epithelium (RPE) and outer retina.[1] The second major clinical phenotype, neovascular AMD, is manifested by the invasion of choroidal neovascularization (CNV) into the sub-RPE and subretinal space. In neovascular AMD, there are leakage, hemorrhage, and scarring, with progressive loss of the RPE and overlying photoreceptors.[2] Intravitreal injections of agents directed against vascular endothelial growth factor have changed the course of neovascular AMD from expected severe vision loss to stabilization or even visual acuity improvement for many, but not all, patients with neovascular AMD.[3-5]

In parallel with these therapeutic advances, ocular imaging has improved. Spectral-domain optical coherence tomography (SD-OCT) has become an essential tool for the diagnosis and monitoring of patients with AMD. The high scanning speed of SD-OCT made it possible to reduce artifacts associated with eye motion, decrease noise in images through the averaging of multiple scans,[6] and acquire 3-dimensional data sets, which can be used to evaluate alteration of tissue structure.[7] Accurate interpretation of OCT images is indispensable to avoid unnecessary treatments for patients with AMD. However, tomographic abnormalities of AMD have not been fully characterized because of the complex morphology and a lack of correlative histologic studies. In this study, we showed a newly recognized outer retinal entity (a hyperreflective material above the Bruch membrane) in SD-OCT images and suggested a histopathologic correlate.

Methods

We retrospectively reviewed medical records of patients with AMD with severe atrophy due to either CNV or GA. This study had institutional review board approval, complied with the Health Insurance Portability and Accountability Act of 1996, and adhered to the tenets of the Declaration of Helsinki. Patients with AMD examined between November 2012 and November 2013 at Vitreous Retina and Macula Consultants of New York (under the care of R.F.S.) were eligible. All patients provided written informed consent. Patients with CNV secondary to myopia or infective, inflammatory, or hereditary causes were excluded. Other exclusion criteria included high myopia (spherical equivalent <−6 diopters), diabetic retinopathy, previous retinal vascular occlusion, vitreoretinal or glaucoma surgery, macular hole, history of retinal detachment, and central serous chorioretinopathy. Additional exclusionary criteria were media opacities significant enough to affect the quality of imaging.

Demographic data included age, sex, patient's lens status (phakic, pseudophakic, or aphakic), and medical history. Data collection included visual acuity; details of photodynamic therapy; and any intravitreal ranibizumab, bevacizumab, aflibercept, or triamcinolone injections. All patients underwent a comprehensive ophthalmologic examination including best-corrected visual acuity, color fundus photography, fluorescein angiography, and SD-OCT (Spectralis, Heidelberg Engineering) as part of their routine evaluation. We manually measured the thickness of the hyperreflective material at 5 points (fovea, 0.5 mm and 1 mm nasal or temporal to the fovea) by using the digital caliper tool built into the SD-OCT system and calculated the mean thickness of each patient. Some SD-OCT images had volume rendering using the programs ImageJ (version 1.48, National Institute of Mental Health) and Medical Image Processing, Analysis, and Visualization (version 7.01, National Institutes of Health). Surface rendering images and en face images were reconstructed from a data set of serial B-scans (distance between each scan, 12-30 μm). The data were exported from the Heidelberg Spectralis as an XML file, which was then imported into the ImageJ program. The images were straightened in bulk in ImageJ and then saved as a stacked tif file. This file in turn could be read by Medical Image Processing, Analysis, and Visualization, which was used to perform volume rendering. Referring to the infrared reflectance images showing the scanned area, the stacked images of the en face SD-OCT image were registered with fundus photography by matching the shape of the vessels.

The findings evaluated in SD-OCT images were compared with histopathologic findings in donor eyes with GA or CNV. This study used donor eyes accessioned for research from the Alabama Eye Bank. Mean death-to-preservation time was within 3 hours. Although clinical records were available for some eyes and all eyes were subject to ex vivo imaging, AMD case ascertainment was made primarily by histopathologic criteria. Criteria included atrophic RPE, with or without choroidal neovascularization and its sequelae (fibrovascular and fibrocellular scars), with evidence for drusen/basal linear deposit (BLinD) and basal laminar deposit (BLamD) in areas surrounding the atrophy.

Two series of eyes were examined. In a GA-only series, 9 donor eyes preserved by immersion in 4% paraformaldehyde after anterior segment removal were processed for 10-μm cryosections, as previously described,[8,9] and stained with periodic acid–Schiff hematoxylin to highlight carbohydrate residues especially abundant in BLamDs and in the Bruch membrane.[10] Glass slides were reviewed with a ×40 planapochromat objective (numerical aperture, 0.95 objective) and imaged with a charge-coupled device camera (XC-10, Olympus).

A second series of 53 eyes with advanced atrophic or exudative AMD was preserved by immersion in 1% paraformaldehyde and 2.5% glutaraldehyde in 0.1M phosphate buffer after anterior segment removal. Tissue was postfixed using osmium tannic acid paraphenylenediamine to highlight neutral lipids in extracellular AMD-associated lesions. Maculawide high-resolution sections (0.8 μm thick) were collected starting at the superior edge of an 8-mm-diameter full-thickness punch, and sections in the superior perifovea and foveola were stained with toluidine blue. Thicknesses of 21 chorioretinal layers were measured from digital slides created by scanning these sections with the ×40 objective, a robotic microscope stage, and image-stitching software (CellSens; Olympus) as described[11] (visible online at http://projectmacula.cis.uab.edu/). Glass slides were viewed and photographed with

Figure 1. Outer Retinal Corrugations Detected by Spectral-Domain Optical Coherence Tomography in an Eye With Choroidal Neovascularization
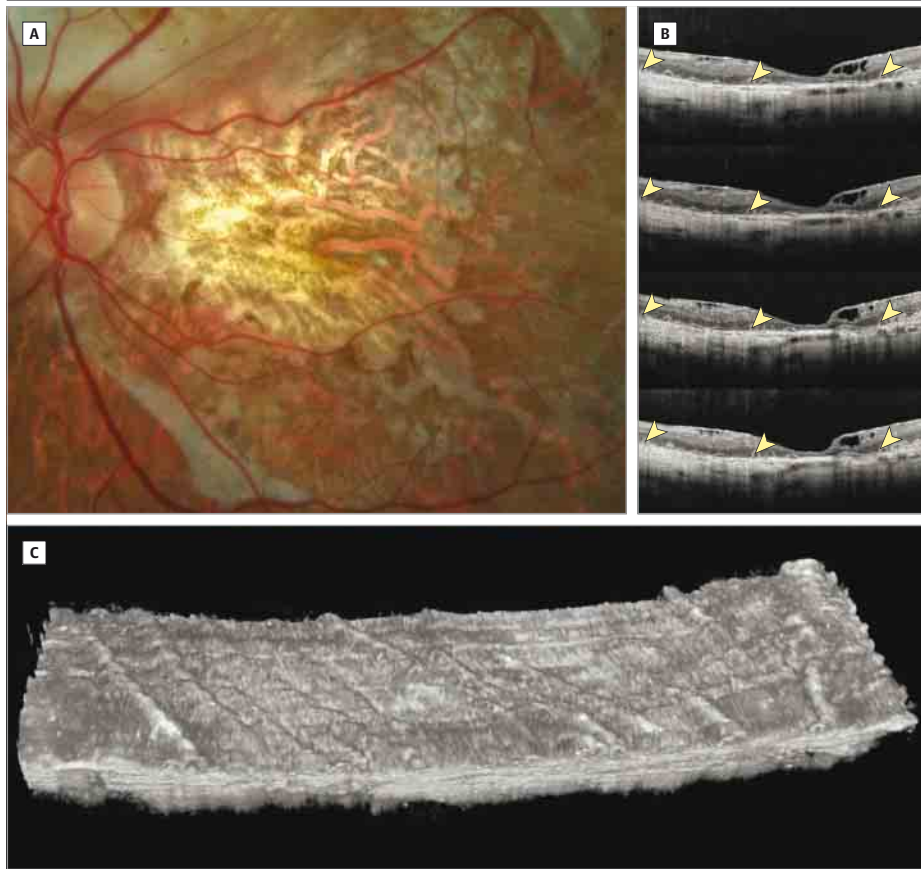
Images of the left eye of a 71-year-old woman with age-related macular degeneration and best-corrected visual acuity of 20/100. A, Fundus photograph shows severe atrophy due to choroidal neovascularization. B, Serial B-scan images (distance between each scan, 30 μm). B-scan images show a continuous curvilinear hyperreflective material (arrowheads) above the tissue, suggesting fibrovascular scar due to choroidal neovascularization. Below the material there is a hyporeflective space. C, A composite surface volume rendering image shows a sheet of the material thrown into folds.

a ×60 oil-immersion planapochromat objective (numerical aperture, 1.4) in parallel with digital sections.

The distinction between BLamD and BLinD was originally made using transmission electron microscopy.[12,13] This distinction can also be made by high-resolution light microscopy using toluidine blue–stained semi-thin sections of tissues prepared for electron microscopy,[11,14] allowing survey of larger samples. In this preparation, the principal components of BLamD are basement membrane proteins that stain blue. The principal component of BLinD is lipoprotein-derived debris[15] (originally called *membranous debris*[12]) that stains gray, tan, or brown. Early and late BLamD are both distinguishable from BLinD, which is an undulating band several micrometers thick between early BLamD and the inner collagenous layer of the Bruch membrane, and by their greater combined thickness, proximity to RPE, distinctive textures, and color.
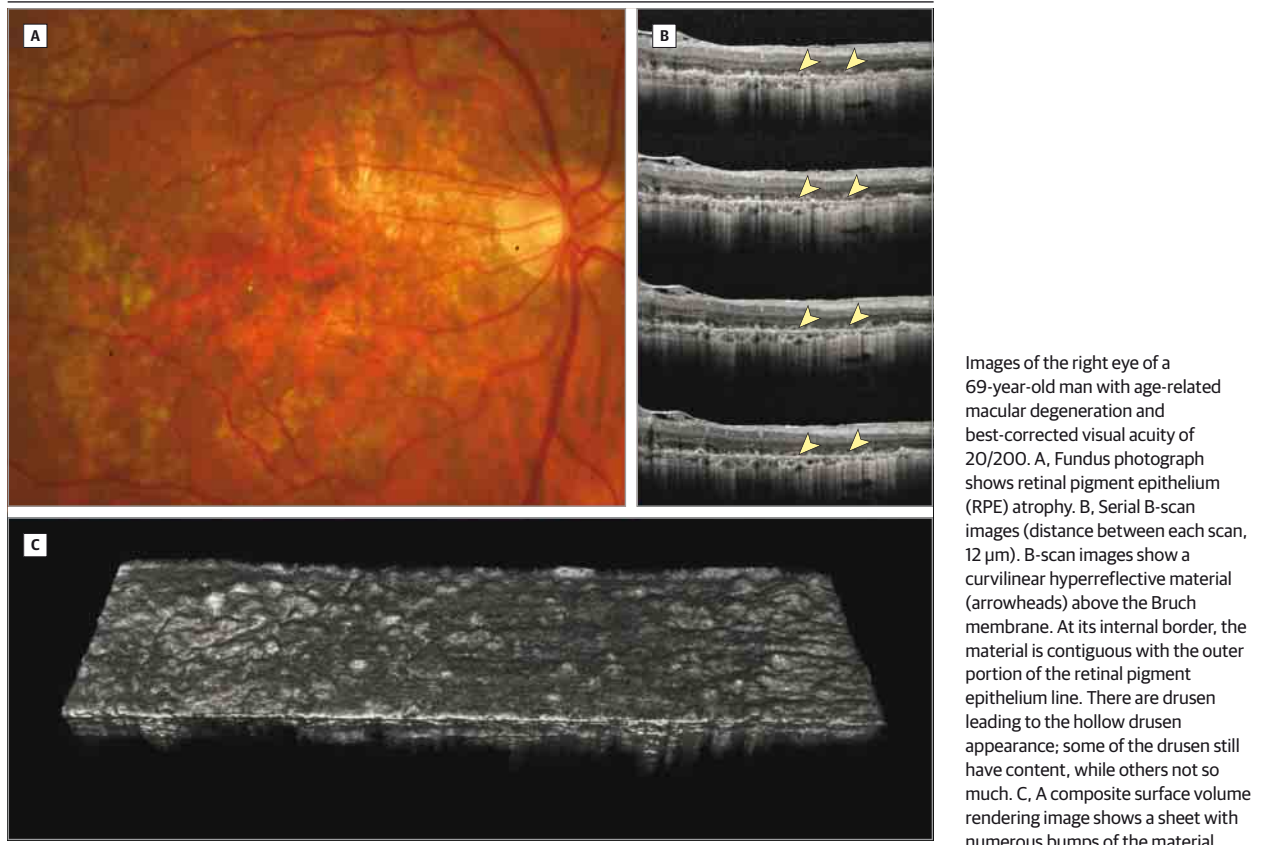
Results

There were 25 eyes of 16 patients with severe atrophy associated with AMD. Patients had a mean (SD) age of 82.7 (7.9) years, 10 (62.5%) of whom were women. Twenty eyes had CNV and 5 eyes had GA. The mean best-corrected visual acuity was 0.800 logMAR (interquartile range, 0.350-1.000 logMAR), which corresponds to a Snellen equivalent of 20/126. The eyes with CNV

were treated with intravitreal injection of ranibizumab in 16 eyes, aflibercept in 7, bevacizumab in 11, and triamcinolone in 2. Photodynamic therapy had been performed in 8 eyes.

A curvilinear hyperreflective material was identified above the Bruch membrane line within the atrophic area in the SD-OCT images (**Figures 1** and **2**, eFigure 1 in Supplement). It lay above the hyperreflective tissue, suggesting fibrovascular scar in CNV eyes (Figure 1), and just above the Bruch membrane line in GA eyes (Figure 2). The mean (SD) thickness of the material was 14.1 (3.6) μm. At its internal border, the material was contiguous with the outer portion of the RPE band. Below the material was a relatively hyporeflective space. Composite surface volume rendering images revealed that the material seen was thrown into folds in more widespread cases with atrophy following CNV (Figure 1). These folds were only seen within the atrophic area (eFigure 1 in Supplement), and their orientations were different from those of the underlying large choroidal vessels (Figure 1 and eFigure 1 in Supplement). In eyes with GA, there were drusen leading to a hollow appearance under the drusen; some of the drusen still had some reflective material while others did not (Figure 2). Composite surface volume rendering images showed a sheet with numerous bumps in the material (Figure 2).

Basal laminar deposit in advanced AMD eyes with intact RPE is continuous and frequently exhibits sublayers of early and late forms,[12] as seen by high-resolution histology

Figure 2. Outer Retinal Corrugations Detected by Spectral-Domain Optical Coherence Tomography in an Eye With Geographic Atrophy

Images of the right eye of a 69-year-old man with age-related macular degeneration and best-corrected visual acuity of 20/200. A, Fundus photograph shows retinal pigment epithelium (RPE) atrophy. B, Serial B-scan images (distance between each scan, 12 μm). B-scan images show a curvilinear hyperreflective material (arrowheads) above the Bruch membrane. At its internal border, the material is contiguous with the outer portion of the retinal pigment epithelium line. There are drusen leading to the hollow drusen appearance; some of the drusen still have content, while others not so much. C, A composite surface volume rendering image shows a sheet with numerous bumps of the material.

(eFigure 2 in Supplement). Basal laminar deposit separates RPE from the true basal lamina, which is visible only by electron microscopy. Late BLamD is scalloped (convex toward the RPE), located close to the RPE, and has little lipoprotein-derived debris within it. Early BLamD is palisadelike, located close to the Bruch membrane, and has noticeable lipoprotein-derived debris within it, apparently in transit to the Bruch membrane.[16] Basal linear deposit is an undulating band several micrometers thick between early BLamD and the inner collagenous layer of the Bruch membrane (in the sub-RPE space).

Review of histopathologic findings of eyes with advanced GA and CNV revealed an undulating layer of BLamD persisting in an area of RPE atrophy. In 7 of 9 specimens of GA stained with periodic acid–Schiff hematoxylin, the rippling was remarkable (**Figure 3**). The BLamDs were seen external to RPE peripheral to the atrophic zone and then continued into the area of RPE loss as an undulating layer (Figure 3A). Five of these GA eyes had a widespread area of undulating BLamD. Between this persistent BLamD and the Bruch membrane were processes of apparent retinal origin, with occasional nodules of calcified druse material (Figure 3B and C).

In 36 of 40 eyes with CNV (mean [SD] age, 85.4 [5.4] years) and 10 of 13 eyes with GA (mean [SD] age, 85.6 [7.1] years), persistent BLamDs were observed in the area of RPE loss (**Figure 4** and eFigure 3 in Supplement). Some described features fall

below clinical detectability with current instrumentation and are presented here to guide future examination using higher-resolution images when they are available. Compared with BLamD external to intact RPE in advanced AMD eyes (eFigure 2 in Supplement), persistent BLamD in advanced AMD eyes with absent RPE is generally thin and tattered (Figure 4, eFigure 3A-D in Supplement), although sublayers of early and late forms are recognizable. Persistent BLamD within corrugations is thick and curved, with concavities open toward the Bruch membrane (Figure 4, eFigure 3A and D in Supplement).

Within the concavities created by undulating deposits in GA eyes are cells of retinal origin (eFigure 3B in Supplement) and fragments of calcified drusen (eFigure 3C in Supplement). Müller cells undermine and clear the deposits (eFigure 3B in Supplement). Within the concavities created by undulating deposits in neovascular AMD eyes are CNV, macrophages, and aggregations of unidentified cells overlying fibrovascular scar (Figure 4 and eFigure 3D in Supplement).

In 53 eyes with advanced AMD, thicknesses of persistent BLamD were measured at 565 locations. Mean thickness was 9.5 μm (interquartile range, 4.4-11.3 μm). Five percent of thicknesses were greater than 25 μm (eFigure 3E in Supplement), all in neovascular AMD eyes, and these frequently exhibited sublayers of early and late BLamD. The thickest persistent BLamD observed was 71.9 μm.

Discussion

Basal laminar deposit is found between the RPE and its basement membrane,[12-15,17-25] is a histopathologic correlate of AMD, and is a marker of RPE stress.[24] There is progressive accumulation of BLamD in early AMD and it persists in late AMD specimens in histologic studies,[12-15,17,20,25] enabling a distinction between scars in subretinal and sub-RPE compartments even when RPE is atrophied.[13] Using SD-OCT, we found an undulating sheet of hyperreflective material above the Bruch membrane contiguous with the back surface of the band ascribed to the RPE, which then extended into neighboring regions devoid of RPE. We have termed this entity *outer retinal corrugations* in keeping with its appearance. Comparison of the OCT appearance of this structure with histologic specimens showed the outer retinal corrugations seen in OCT may correspond to histologic BLamD.

Basal laminar deposits consist primarily of basement membrane proteins with a distinct fibrous long-spacing collagen embedded within it.[24,26,27] The early form of BLamD appears as a discontinuous thin fibrous layer, and the late form of BLamD, which appears concomitantly with progression of RPE degeneration, elaborates a multilayered diffuse wavy thickening internal to the inner collagenous layer of the Bruch membrane.[13,20,25,28] In the current study, BLamD was seen under the RPE and persisted in the absence of RPE and photoreceptors in advanced late AMD. The mean thickness of the persistent BLamD was 9.5 μm in the histologic specimens, which is greater than the axial resolution of current SD-OCT systems, and some of the BLamD accumulations were many times

Figure 3. Histopathology of a Donor Eye of a 90-Year-Old Woman With Geographic Atrophy Associated With Age-Related Macular Degeneration
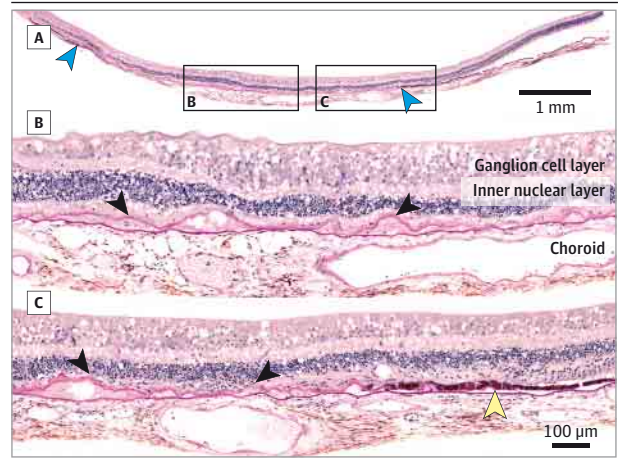
Ten-μm-thick cryosections were stained with periodic acid–Schiff hematoxylin, as described.[8] A, A section through the area with retinal pigment epithelium (RPE) atrophy. The boxes indicate areas shown in panels B and C. The RPE atrophy is seen between the blue arrowheads. The optic nerve head is at the left. B and C, High-magnification images revealing a rippled layer of pink-stained persistent basal laminar deposit (BLamD) (arrowheads) in an area of RPE atrophy. The Bruch membrane is straight and also stained pink. Scale bar applies to B and C. B, Calcific nodules and isolated cells are found external to undulating, persistent BLamD (arrowheads). The outer nuclear layer is absent. C, The yellow arrowhead indicates intact, although dysmorphic, RPE with underlying BLamD. This deposit continues into the area of RPE loss as an undulating layer (black arrowheads). Note that BLamDs persist in spite of the (near) absence of outer nuclear layer, photoreceptor layer, and RPE. A few cone nuclei overlie the deposit near the right black arrowhead.

Figure 4. High-Resolution Histology Sections Showing Outer Retinal Corrugation in Advanced Age-Related Macular Degeneration
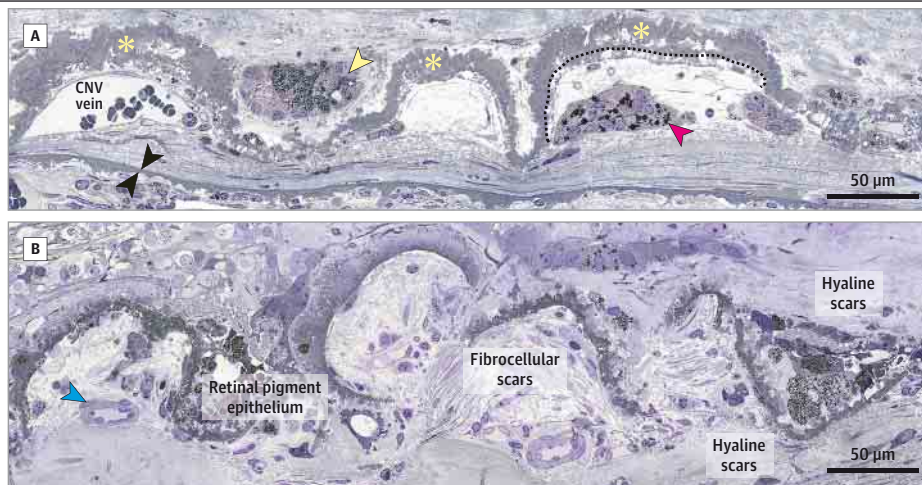
Tissues were postfixed with osmium tannic acid paraphenylenediamine, and 0.8-μm-thick sections were stained with toluidine blue. A, Neovascular age-related macular degeneration in an 81-year-old woman. Highly corrugated layer of thick, persistent basal laminar deposit (asterisks) between a fibrocellular scar in the subretinal space (above) and sub–retinal pigment epithelium (RPE) space (below). The dotted line separates sublayers of late (above) and early (below) forms of basal laminar deposit. In the corrugation concavities, and overlying fibrovascular scar, are a choroidal neovascularization (CNV) vein with erythrocytes and a multicellular aggregate with spherical melanosomes (red arrowhead). Internal to the corrugations and entombed by scar are RPE cells with green-stained lipofuscin (yellow arrowhead). The Bruch membrane is indicated by black arrowheads. Choriocapillaris endothelium has been replaced by presumed macrophages. B, Neovascular age-related macular degeneration in an 88-year-old man. Highly corrugated and discontinuous layer of thick persistent basal laminar deposit separates scars in the subretinal and sub-RPE compartments. Hyaline and fibrocellular scars are visible. Entombed RPE is present internal to a valley between corrugations. The blue arrowhead indicates a small arteriole.

Figure 5. Proposal as to How the Basal Laminar Deposit (BLamD) Can Look Folded and Possible Mechanisms of Formation of the Clinical Picture
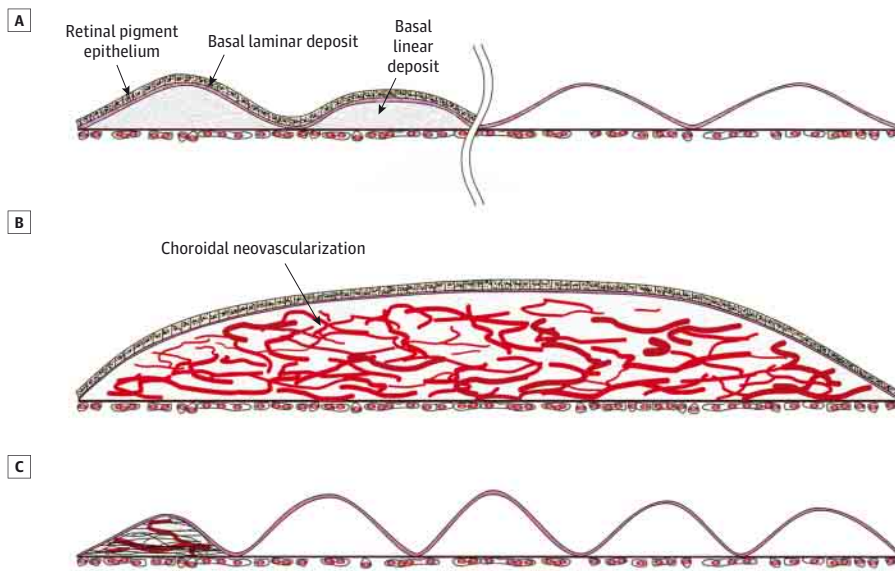
A, The left side of the image shows intact retinal pigment epithelium with BLamD (pink material). There is basal linear deposit forming a druse. The right side shows an area where geographic atrophy has developed, with loss of the retinal pigment epithelium and the basal linear deposit. The BLamD remains. B, A case of choroidal neovascularization shows the retinal pigment epithelium and neovascular tissue. C, Some cases of choroidal neovascularization regress, leaving minimal scarring but have extensive tissue loss. The remaining BLamD, which was formed when the choroidal neovascularization formed, has more surface area than the available space. Therefore, the BLamD is thrown into folds.

thicker. In the SD-OCT sections, the thickness was measured to be 14.1 μm, which is actually quite similar to the histologic value given the axial point spread function of SD-OCT.[29] External to persistent BLamD, there was amorphous collections and evidence in areas of cellular processes, possibly of Müller cell origin. In eyes with neovascular AMD, persistent undulating BLamD lay over CNV and fibrocellular proliferation. In both instances, there is a physical separation of the BLamD from the Bruch membrane, offering the possibility of optical differentiation using OCT. However, until now, few reports have identified BLamD clinically using any in vivo imaging modalities.

Using SD-OCT, Fleckenstein et al[30] described elevations or accumulations of highly reflective material within the atrophic area in eyes with GA and postulated that these alterations may represent residual sub-RPE deposits and regressing drusen. In a separate publication, Fleckenstein and colleagues[31] described the imaging characteristics of a rapidly progressive form of GA and stated that these eyes showed a splitting of the band ascribed to the RPE. This band consisted of a highly reflective inner portion and a lesser reflecting outer portion. The outer portion appeared to extend on the Bruch membrane into areas devoid of RPE. There were no undulations described in the area with intact RPE and none shown or described in the areas devoid of RPE. It is possible that this finding was consistent with BLamD. In the current study, using SD-OCT with volume rendering, the hyperreflective material in the outer retina was thrown into folds in more widespread cases with atrophy following CNV or was seen as a sheet with numerous bumps in eyes with GA. These findings are consistent with the rippled layer of BLamD that persisted in areas with atrophy due to CNV or GA seen in histological specimens. In addition, at the internal border, the hyperreflective material was contiguous with the outer portion of the RPE band, corresponding to the anatomical location of the BLamD.[12,20,25]

Outer retinal corrugations were seen only in areas with atrophy associated with CNV or GA. Histological specimens revealed that the BLamD lay just adjacent to the RPE in areas with intact RPE both in GA eyes and CNV eyes. Thus, the visualization of the hyperreflective material on SD-OCT suggests that, at least in some AMD eyes, the OCT-designated RPE band may be more than just RPE (ie, RPE with sub-RPE deposits such as BLamD). The thickness of the outer band visualized in SD-OCT is thicker than that of the RPE monolayer itself, supporting this contention.[29]

Figure 5 shows possible mechanisms by which BLamD could create the observed OCT picture. Outside the areas of GA, BLinD and soft drusen form beneath intact RPE and BLamD. In an area where GA has developed, the BLamD remains in spite of a loss of the RPE and the BLinD. In some cases of neovascular AMD, CNV regresses, leaving minimal scarring. The remaining BLamD, which was formed when the CNV developed, would have more surface area than the available space, thus the BLamD would be thrown into folds. This mechanism of outer retinal corrugations in eyes with CNV could potentially also be applied following the regression of drusenoid pigment epithelial detachments to GA eyes.

Conclusions

This study has several limitations. In addition to the retrospective nature of the study, there was requisite speculation about the exact correlate in the histologic specimens because they were of different participants. However, visualizing the undulating band by SD-OCT is common in late-stage AMD eyes and the location is precisely where the BLamD is seen, also commonly, in histologic specimens. These characteristics and the similar morphologic features suggest that outer retinal cor-

rugations represent persistent BLamD. Expansion of our ability to interpret increasing fine and subtle attributes brings us closer to the goal of in vivo histologic analysis of the eye by OCT. Indeed, with OCT signatures now available, longitudinal study in patient populations[32] can combine with molecular analysis of animal models of thick BLamD[24,33,34] to elucidate the importance of this understudied lesion for AMD

progression. The finding of outer retinal corrugation in eyes with CNV does not necessarily mean there is exudation or leakage; as a consequence, these patients do not need treatment based on this solitary finding. Recognition of this feature will allow some patients with AMD to avoid unnecessary interventions and may also lead to further understanding of AMD pathology.

REFERENCES

1. Klein ML, Ferris FL III, Armstrong J, et al; AREDS Research Group. Retinal precursors and the development of geographic atrophy in age-related macular degeneration. *Ophthalmology*. 2008;115 (6):1026-1031.

2. Kumar N, Mrejen S, Fung AT, Marsiglia M, Loh BK, Spaide RF. Retinal pigment epithelial cell loss assessed by fundus autofluorescence imaging in neovascular age-related macular degeneration. *Ophthalmology*. 2013;120(2):334-341.

3. Rosenfeld PJ, Brown DM, Heier JS, et al; MARINA Study Group. Ranibizumab for neovascular age-related macular degeneration. *N Engl J Med*. 2006;355(14):1419-1431.

4. Brown DM, Kaiser PK, Michels M, et al; ANCHOR Study Group. Ranibizumab versus verteporfin for neovascular age-related macular degeneration. *N Engl J Med*. 2006;355(14):1432-1444.

5. Brown DM, Michels M, Kaiser PK, Heier JS, Sy JP, Ianchulev T; ANCHOR Study Group. Ranibizumab versus verteporfin photodynamic therapy for neovascular age-related macular degeneration: two-year results of the ANCHOR Study. *Ophthalmology*. 2009;116(1):57-65.e5.

6. Kanagasingam Y, Bhuiyan A, Abràmoff MD, Smith RT, Goldschmidt L, Wong TY. Progress on retinal image analysis for age related macular degeneration. *Prog Retin Eye Res*. 2014;38:20-42.

7. Keane PA, Patel PJ, Liakopoulos S, Heussen FM, Sadda SR, Tufail A. Evaluation of age-related macular degeneration with optical coherence tomography. *Surv Ophthalmol*. 2012;57(5):389-414.

8. Vogt SD, Curcio CA, Wang L, et al. Retinal pigment epithelial expression of complement regulator CD46 is altered early in the course of geographic atrophy. *Exp Eye Res*. 2011;93(4):413-423.

9. Rudolf M, Vogt SD, Curcio CA, et al. Histologic basis of variations in retinal pigment epithelium autofluorescence in eyes with geographic atrophy. *Ophthalmology*. 2013;120(4):821-828.

10. van der Schaft TL, Mooy CM, de Bruijn WC, Oron FG, Mulder PG, de Jong PT. Histologic features of the early stages of age-related macular degeneration. A statistical analysis. *Ophthalmology*. 1992;99(2):278-286.

11. Curcio CA, Messinger JD, Sloan KR, McGwin G, Medeiros NE, Spaide RF. Subretinal drusenoid deposits in non-neovascular age-related macular degeneration: morphology, prevalence, topography, and biogenesis model. *Retina*. 2013;33 (2):265-276.

12. Sarks JP, Sarks SH, Killingsworth MC. Evolution of geographic atrophy of the retinal pigment epithelium. *Eye (Lond)*. 1988;2(pt 5):552-577.

13. Green WR, Enger C. Age-related macular degeneration histopathologic studies: the 1992 Lorenz E. Zimmerman Lecture. *Ophthalmology*. 1993;100(10):1519-1535.

14. Curcio CA, Millican CL. Basal linear deposit and large drusen are specific for early age-related maculopathy. *Arch Ophthalmol*. 1999;117(3):329-339.

15. Curcio CA, Johnson M, Huang JD, Rudolf M. Aging, age-related macular degeneration, and the response-to-retention of apolipoprotein B-containing lipoproteins. *Prog Retin Eye Res*. 2009;28(6):393-422.

16. Curcio CA, Presley JB, Millican CL, Medeiros NE. Basal deposits and drusen in eyes with age-related maculopathy: evidence for solid lipid particles. *Exp Eye Res*. 2005;80(6):761-775.

17. Sarks SH. Ageing and degeneration in the macular region: a clinico-pathological study. *Br J Ophthalmol*. 1976;60(5):324-341.

18. Chen L, Miyamura N, Ninomiya Y, Handa JT. Distribution of the collagen IV isoforms in human Bruch's membrane. *Br J Ophthalmol*. 2003;87(2): 212-215.

19. Knupp C, Chong NH, Munro PM, Luthert PJ, Squire JM. Analysis of the collagen VI assemblies associated with Sorsby's fundus dystrophy. *J Struct Biol*. 2002;137(1-2):31-40.

20. Curcio CA, Presley JB, Malek G, Medeiros NE, Avery DV, Kruth HS. Esterified and unesterified cholesterol in drusen and basal deposits of eyes with age-related maculopathy. *Exp Eye Res*. 2005; 81(6):731-741.

21. Grossniklaus HE, Miskala PH, Green WR, et al. Histopathologic and ultrastructural features of surgically excised subfoveal choroidal neovascular lesions: Submacular Surgery Trials report No. 7. *Arch Ophthalmol*. 2005;123(7):914-921.

22. Kuntz CA, Jacobson SG, Cideciyan AV, et al. Sub-retinal pigment epithelial deposits in a dominant late-onset retinal degeneration. *Invest Ophthalmol Vis Sci*. 1996;37(9):1772-1782.

23. Milam AH, Curcio CA, Cideciyan AV, et al. Dominant late-onset retinal degeneration with regional variation of sub-retinal pigment epithelium deposits, retinal function, and photoreceptor degeneration. *Ophthalmology*. 2000;107(12):2256-2266.

24. Marmorstein LY, McLaughlin PJ, Peachey NS, Sasaki T, Marmorstein AD. Formation and progression of sub-retinal pigment epithelium deposits in Efemp1 mutation knock-in mice: a model for the early pathogenic course of macular degeneration. *Hum Mol Genet*. 2007;16(20):2423-2432.

25. Sarks S, Cherepanoff S, Killingsworth M, Sarks J. Relationship of basal laminar deposit and membranous debris to the clinical presentation of early age-related macular degeneration. *Invest Ophthalmol Vis Sci*. 2007;48(3):968-977.

26. Knupp C, Munro PM, Luther PK, Ezra E, Squire JM. Structure of abnormal molecular assemblies (collagen VI) associated with human full thickness macular holes. *J Struct Biol*. 2000;129(1):38-47.

27. Reale E, Groos S, Eckardt U, Eckardt C, Luciano L. New components of 'basal laminar deposits' in age-related macular degeneration. *Cells Tissues Organs*. 2009;190(3):170-181.

28. van der Schaft TL, Mooy CM, de Bruijn WC, Bosman FT, de Jong PT. Immunohistochemical light and electron microscopy of basal laminar deposit. *Graefes Arch Clin Exp Ophthalmol*. 1994;232(1): 40-46.

29. Spaide RF, Curcio CA. Anatomical correlates to the bands seen in the outer retina by optical coherence tomography: literature review and model. *Retina*. 2011;31(8):1609-1619.

30. Fleckenstein M, Charbel Issa P, Helb HM, et al. High-resolution spectral domain-OCT imaging in geographic atrophy associated with age-related

macular degeneration. *Invest Ophthalmol Vis Sci*. 2008;49(9):4137-4144.

31. Fleckenstein M, Schmitz-Valckenberg S, Martens C, et al. Fundus autofluorescence and spectral-domain optical coherence tomography characteristics in a rapidly progressing form of geographic atrophy. *Invest Ophthalmol Vis Sci*. 2011; 52(6):3761-3766.

32. Moussa K, Lee JY, Stinnett SS, Jaffe GJ. Spectral domain optical coherence tomography-determined morphologic predictors of age-related macular degeneration-associated geographic atrophy progression. *Retina*. 2013;33(8):1590-1599.

33. Wavre-Shapton ST, Tolmachova T, Lopes da Silva M, Futter CE, Seabra MC. Conditional ablation of the choroideremia gene causes age-related changes in mouse retinal pigment epithelium [published correction appears in *PLoS One*. 2013;8(5)]. *PLoS One*. 2013;8(2):e57769.

34. Garland DL, Fernandez-Godino R, Kaur I, et al. Mouse genetics and proteomic analyses demonstrate a critical role for complement in a model of DHRD/ML, an inherited macular degeneration. *Hum Mol Genet*. 2014;23(1):52-68.

OPHTHALMIC IMAGES

Multimodal Imaging of Intracameral Foreign Body

Jaidrath Kumar, MS; Aniruddha Agarwal, MBBS; Jagat Ram, MS
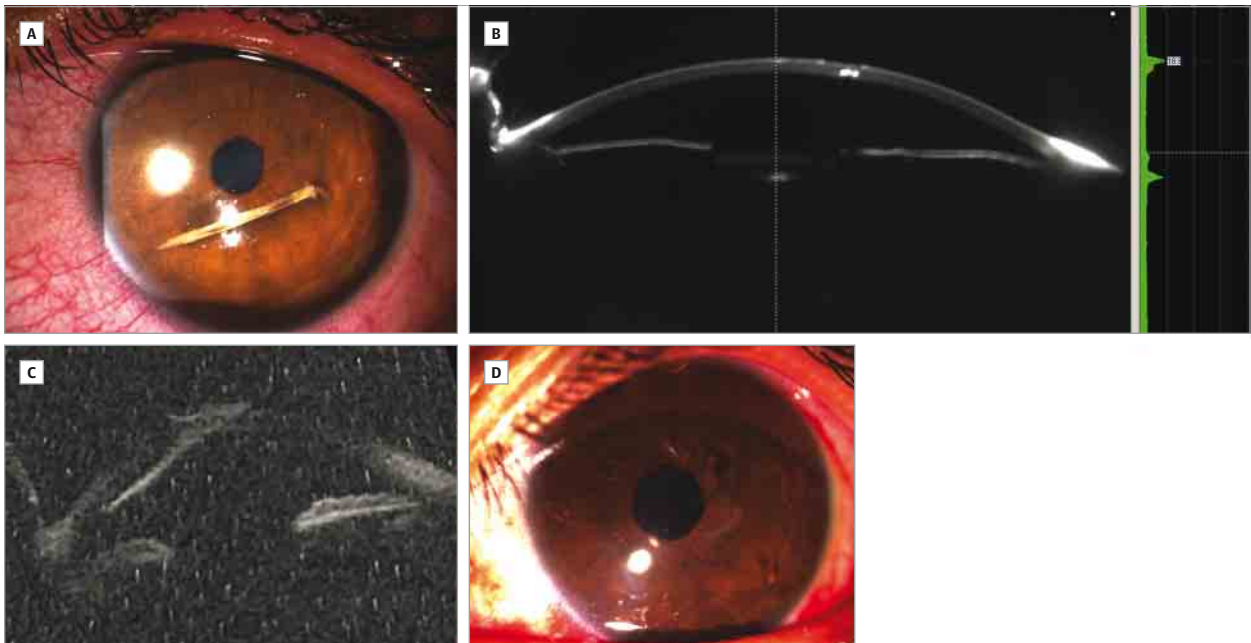
A, An 8-year-old girl presented with trauma with a wooden stick. B, Scheimpflug imaging demonstrates the site of corneal entry. C, Ultrasound biomicroscopy shows its precise intracameral location. D, After removal of the foreign body, there was a well-formed anterior chamber.